

Suzaku Observations of the Prototype Wind-Blown Bubble NGC 6888

Svetozar A. Zhekov^{1,3}, and Sangwook Park²

ABSTRACT

We present an analysis of the *Suzaku* observations of the prototype wind-blown bubble NGC 6888 which is based both on use of standard spectral models and on a direct comparison of theoretical models with observations. The X-ray spectra of NGC 6888 are soft and most of the X-rays are in the (0.3 - 1.5 keV) energy range. But, hard X-rays (1.5 - 4.0 keV) are also detected ($\sim 10\%$ of the observed flux). The corresponding spectral fits require a relatively cool plasma with $kT \leq 0.5$ keV but much hotter plasma with temperature $kT \geq 2.0$ keV is needed to match the observed hard X-ray emission. We find no appreciable temperature variations within the hot bubble in NGC 6888. The derived abundances (N, O, Ne) are consistent with those of the optical nebula. This indicates a common origin of the X-ray emitting gas and the outer cold shell: most of the X-ray plasma (having non-uniform spatial distribution: clumps) has flown into the hot bubble from the optical nebula. If the electron thermal conduction is efficient, this can naturally explain the relatively low plasma temperature of most of the X-ray emitting plasma. Alternatively, the hot bubble in NGC 6888 will be adiabatic and the cold clumps are heated up to X-ray temperatures likely by energy exchange between the heavy particles (hot ions diffusing into the cold clumps).

Subject headings: ISM: individual objects (NGC 6888) — ISM: bubbles — X-rays: ISM — shock waves

¹JILA, University of Colorado, Boulder, CO 80309-0440, USA; zhekovs@colorado.edu

²Department of Physics, Box 19059, University of Texas at Arlington, Arlington, TX 76019; s.park@uta.edu

³On leave from Space Research Institute, Sofia, Bulgaria

1. Introduction

Optical nebulosities trace large cavities around early-type stars (O, Of and Wolf-Rayet, WR) that are formed as the high-speed wind sweeps up ambient interstellar gas and compresses it into a thin shell. The flow pattern, resulting from this interaction, was first recognized by Pikelner (1968) and consists of two regions of shocked gas: one corresponding to the shocked stellar wind and the other to shocked interstellar gas. The two regions are separated by a contact discontinuity and the hot interior gas can cool via thermal conduction across the interface. Because of its high temperature, the interior of the wind-blown bubbles (WBB) is expected to emit in X-rays.

In 1970s and 1980s, analytical solutions for the WBB structure were derived that revealed details in the physics of these interesting objects. For a review of the analytical works and the related physical ideas see Dyson (1981) and McCray (1983). It should be noted that the most complete (semi-)analytical study of the WBB structure was presented in Weaver et al. (1977). With the increasing computing power, the numerical hydrodynamic simulations became a powerful tool for studying the physics of these objects. The first numerical modeling of WBB was done by Falle (1975) and later on details of the adiabatic, radiative and conductive WBB were studied numerically (e.g., Rozyczka 1985; Rozyczka & Tenorio-Tagle, 1985a,b,c; Brighenti & D’Ercole, 1995a,b, 1997; D’Ercole 1992; Garcia-Segura & Mac Low 1995; Garcia-Segura et al. 1996a; Garcia-Segura et al. 1996b; Zhekov & Myasnikov 1998, 2000). Thanks to numerical simulations, it was found that the WBB are subject to numerous dynamic instabilities. These simulations also allowed a much more complete and complex physical picture be explored, namely, by following various phases of the WBB evolution when the wind of the central stars varies with time (for details see Garcia-Segura et al. 1996a; Garcia-Segura et al. 1996b).

Observational properties of the optical nebula in WBB were described in detail in the early works of Chu et al. (1983 and the references therein) and Lozinskaya (1982; see also the book by Lozinskaya 1993 for an observational review). But, it should be emphasized that the physics of the hot interior (hot bubble) of a wind-blown bubble is a cornerstone in the entire physical picture of these objects. This is so since the hot bubble is the region where the stellar wind energy is stored and subsequently used for driving the entire structure. From such a point of view, X-ray observations of WBB are very important because they can provide us with details about the physical conditions in the hot bubble.

The first successful X-ray detection of a WBB was that of NGC 6888 by *Einstein* (Bochkarev 1988). It was found that the X-ray emission from NGC 6888 is characterized by a plasma temperature $kT = 0.28 - 0.8$ keV (90% confidence interval), or $T = 3.2 - 9$ MK. *ROSAT* observations were sensitive to cooler plasma and yielded a characteristic

temperature $T \approx 2$ MK. They showed that the X-ray emission arises primarily in filament like structures (Wrigge et al. 1994). *ASCA* observations suggested that even hotter plasma at $T \approx 8$ MK might be present in the bubble interior (Wrigge et al. 2005). Preliminary results from a recent Chandra observation, *which covered only the northeast part* of NGC 6888, detected plasma with a temperature of $T \approx 2 - 3$ MK and possible nitrogen enrichment (Chu et al. 2006). Similar soft X-ray spectra were detected for another WBB, S308, with *ROSAT* (Wrigge 1999) and *XMM-Newton* (Chu et al. 2003). Unfortunately, none of these data provided us with solid grounds to draw a firm conclusion about the physical mechanism responsible for the X-ray emission from WBB. Obviously, the X-ray emitting plasma in the hot bubble has a moderate temperature (considerably lower than the one expected from a shock with velocity equal to that of the stellar wind) and the reason for this could be that the thermal conduction operates efficiently in the hot interior. But, it is necessary to have solid observational arguments that support or rule out such a theoretical expectation.

This was the basic motivation for the recent *Suzaku* observations of NGC 6888 which covered the entire object and provided us with the X-ray spectra having good photon statistics. We report here the results from our analysis of these data. The paper is organized as follows. We give some basic information about the WBB NGC 6888 in Section 2. In Section 3, we briefly review the *Suzaku* observations. In Section 4, we present results from the global spectral models. In Section 5, we discuss the origin of the hot gas in NGC 6888. In Section 6, we discuss our results and we present our conclusions in Section 7.

2. The Wind-Blown Bubble NGC 6888

The nebula NGC 6888 around the Wolf-Rayet star WR 136 is the prototype of a broad class of ring nebulae around stars with strong stellar winds. The size of the optical nebula is $12' \times 18'$ and its expansion velocity is 75 km s^{-1} (Chu et al. 1983). The distance to NGC 6888 (WR 136) is $d = 1.26 \text{ kpc}$ (van der Hucht 2001), thus, the dynamical age of the object is 30,000 years. The observed X-ray flux in the *ROSAT* PSPC band is $1.2 \times 10^{-12} \text{ erg cm}^{-2} \text{ s}^{-1}$ with an X-ray absorption column density of $N_H = 3.2 \times 10^{21} \text{ cm}^{-2}$ (Wrigge et al. 1994). A larger flux value of $1.86 \times 10^{-12} \text{ erg cm}^{-2} \text{ s}^{-1}$ is obtained from the *ACSA* observations of this object (Wrigge et al. 2005).

The central star, WR 136, is a WN6 star (van der Hucht 2001) with stellar wind parameters $V_{wind} = 1600 \text{ km s}^{-1}$ (Prinja et al. 1990) and $\dot{M} = 1.5 \times 10^{-5} M_{\odot} \text{ yr}^{-1}$. For the mass-loss rate, we used the result for WR 136 derived by Abbott et al. (1986), $\log \dot{M} = -4.5 M_{\odot} \text{ yr}^{-1}$ for $d = 1.8 \text{ kpc}$ and $V_{wind} = 2000 \text{ km s}^{-1}$, and corrected it for the values of the wind velocity and distance adopted here. We made use of the general

dependence $\dot{M} \propto V_{wind} d^{1.5}$ for the mass-loss values derived from the radio observations (Panagia & Felli 1975; Wright & Barlow 1975).

3. Observations and Data Reduction

NGC 6888 was observed with *Suzaku* in two runs: June 4 and November 16, 2009, centered on the North-East and South-West parts of this object thus covering the entire optical nebula. The basic data for our analysis are those from the three active X-ray Imaging Spectrometers (XIS) on-board *Suzaku*. We note that one of them (XIS1) is back-illuminated while the other two (XIS0, XIS3) are front-illuminated CCDs which allows the extracted spectra from units XIS0 and XIS3 be combined for further analysis¹. We extracted X-ray spectra of NGC 6888 from the filtered and screened pipeline events files using the 3×3 and 5×5 observational modes² which resulted in 88.8 ksec and 77.3 ksec effective exposures for the June and November observations, respectively. The total number of source counts in the (0.3 - 4 keV) energy band are 5403 (XIS1) and 4838 (XIS0+XIS3) for the North-East half; 4330 (XIS1) and 3413 (XIS0+XIS3) for the South-West half of NGC 6888. For the current analysis, we extracted one total and two subregion spectra for each of the observed parts of NGC 6888. The corresponding X-ray images as well as source and background regions for the spectral extraction are shown in Fig. 1. The circles in red denote the regions around bright point sources (No. 5, 6 and 7 in Table 4 of Wrigge et al. 1994) that were excluded from the spectral extraction. We note that source No.5 is in fact the central star (WR 136) in the nebula. Since it is not a strong X-ray source (Skinner et al. 2010), the presence of a near by point source (No.6) and the large PSF of *Suzaku* telescopes prevents extraction of valuable information on its X-ray emission. Despite the large ‘pixel’ of *Suzaku* images, Figure 1 shows that the X-rays of NGC 6888 originate from region *inside* the optical nebula and their spatial distribution is *not* uniform (e.g., indicating clump like structures).

We adopted the current calibration database for *Suzaku*, XIS (20100123) and XRT (20080709), to generate the corresponding response matrices and ancillary response files. We made use of standard as well as custom models in version 11.3.2 of XSPEC (Arnaud 1996) for the spectral analysis in this study.

Finally, to facilitate comparisons of the new results on NGC 6888 with those from the

¹ see The *Suzaku* Data Reduction Guide: <http://heasarc.gsfc.nasa.gov/docs/suzaku/analysis/abc/>

² In the 3×3 and 5×5 editing modes, all the pulse heights of the corresponding 9 and 25 pixels centered at the event center are sent to the telemetry. The data for each mode come from different times which effectively increases the exposure time. See http://heasarc.gsfc.nasa.gov/docs/astroe/prop_tools/suzaku_td

previous X-ray observations of this object, we mention a few basic characteristics of the *Suzaku* observations and similarly for those of *ROSAT* and *ASCA*. The *Suzaku* telescopes have spatial resolution of ~ 2 arcmin (expressed as Half-Power Diameter, or HPD). The XIS detectors operate in the 0.2 – 12 keV energy range. At energies below 1 keV the back-illuminated CCD (XIS1) has much better sensitivity (at least a factor of 2) than the front-illuminated CCDs (XIS0, 3), while their effective area is about the same at higher energies (see § 3 in The *Suzaku* Technical Description, footnote 2). On the other hand³, the energy bandpass and spatial resolution (HPD) were: 0.5 – 12 keV and 2.9 arcmin for *ASCA*; 0.12 – 2.4 keV and ~ 30 arcsec for *ROSAT*.

4. Global Spectral Models

4.1. Soft X-ray Spectra

A general property of the *Suzaku* spectra of NGC 6888 is that they are rather soft and no apparent line features are detected at photon energies ≥ 1.5 keV. Hence, we started our analysis with the X-ray spectra in the (0.3 - 1.5 keV) range (re-binned to have a minimum 100 counts per bin) where most of the X-ray counts ($\sim 90\%$) are found. We adopted the following approach.

We used canonical discrete-temperature plasma models to derive the global properties of the X-ray emitting plasma in the hot bubble of NGC 6888. Since the ionization history of the plasma in the hot bubble is very complex and not well constrained, we considered two limiting cases: models that assume plasma in collisional ionization equilibrium (CIE) or plasma with non-equilibrium ionization (NIE). For consistency in the atomic data, we made use of emission models *vapec* and *vpshock* in XSPEC.

As a first step, we fitted the total spectra of the North-East (combined region 1 and 2 in Fig. 1) and South-West (combined region 3 and 4 in Fig. 1) halves simultaneously (four spectra in total). Although the quality of the *Suzaku* spectra is much better compared to that of the previous studies of the entire object, using *ROSAT* and *ASCA* (Wrigge et al. 1994; Wrigge et al. 2005), we do not find it sufficient to allow us investigate possible variations of the X-ray absorption or abundances. Thus, we assumed uniform abundances for the hot

³ For the *ASCA* Technical Description see http://heasarc.gsfc.nasa.gov/docs/asca/asca_nra06/appendix_e/appendix_e.html. For the *ROSAT* Technical Description see <http://heasarc.gsfc.nasa.gov/docs/rosat/ruh/handbook/> and <http://heasarc.gsfc.nasa.gov/docs/journal/pspc2.html>

plasma in NGC 6888 and its X-ray emission is subject to the same interstellar absorption. These were free parameters in our fits. As a basic set of abundances, we adopted the solar abundances of Anders & Grevesse (1989). We varied only the N, O, Ne, Mg and Fe abundances in the spectral fits since these are the elements that provide most of the X-rays in the (0.3 - 1.5 keV) energy range. We also explored a different set of (non-solar) abundances (van der Hucht et al. 1986; see below) that is typical for the stellar wind of the central WN6 star, since this star is the energy source for the hot bubble in NGC 6888.

The results from the global model fits to the entire X-ray spectrum of NGC 6888, assuming uniform plasma temperature, are given in Table 1 and Fig. 2. We note the good quality of the fits and the fact that these fits confirm the early finding that the X-ray plasma in NGC 6888 is relatively ‘cool’ (Bochkarev 1988; Wrigge et al. 1994; Wrigge et al. 2005; Chu et al. 2006). The value of the X-ray absorption is slightly smaller than the one found from the analysis of the entire X-ray spectrum using *ROSAT* and *ASCA* (Wrigge et al. 1994; Wrigge et al. 2005) while the observed flux in the *Suzaku* spectra of NGC 6888 is by 10-20% higher. A possible reason for this could be the quality of the spectra and we note that the total number of counts of the *Suzaku* spectra was at least one order of magnitude larger than that in the *ROSAT* and *ASCA* spectra of NGC 6888. Thus, we believe that the results from the current analysis are better constrained. For comparison, Figure 2 also shows the background spectra after subtracting the non X-ray background, NXB (the NXB spectra were constructed following the procedure in the *Suzaku* Data Reduction Guide, see footnote 1 in § 3). We see that the source and background spectra are very different (e.g., no N VII emission in the latter). This makes us confident about the derived results, despite the large ‘pixel’ of the *Suzaku* telescopes and the close location of the source and background subtraction regions.

As a next step, we searched for temperature variations of the X-ray plasma in the hot bubble of NGC 6888. For this goal, we used 1T *vpshock* model to fit the individual spectra of region 1 and 2 in the North-East and of region 3 and 4 in the South-West halves (see Fig. 1) simultaneously (eight spectra in total). All the spectra shared the same abundances and X-ray absorption. We note that the derived X-ray absorption ($N_H = 2.40_{-0.38}^{+0.50} \times 10^{21} \text{ cm}^{-2}$) and abundances are consistent (being within 1σ errors) with their values from the spectral model fits with uniform plasma temperature and there is no appreciable variation in the plasma temperature within the hot bubble: $kT = 0.47_{-0.12}^{+0.05}$ (region 1); $0.43_{-0.10}^{+0.13}$ (region 2); $0.43_{-0.09}^{+0.11}$ (region 3); $0.37_{-0.09}^{+0.05}$ (region 4); that is all the values are within the 1σ errors from each other. The same is valid for the observed fluxes in the (0.3 - 1.5 keV) energy range: $F_X = (4.44; 4.69; 4.79 \text{ and } 4.70) \times 10^{-13} \text{ ergs cm}^{-2} \text{ s}^{-1}$ for region 1, 2, 3 and 4, respectively. The observed spectra overlaid with the best-fit 1T shock model ($\chi^2/dof = 196/232$) are shown in Fig. 3. Although the X-ray emission of NGC 6888 originates mostly from a non-

uniform distribution of hot plasma (filaments, clumps; see Wrigge et al. 1994; Wrigge et al. 2005; see also Fig. 1), the properties of the X-ray emitting gas (temperature, flux) are quite uniform through the entire hot bubble. So, the high signal-to-noise *Suzaku* data confirm similar findings already reported from the analysis of the *ROSAT* and *ASCA* observations of NGC 6888 (Wrigge et al. 1994; Wrigge et al. 2005). But, we caution that the almost equal values for the observed flux from regions 1, 2, 3 and 4 do not mean that the plasma emissivity in the hot bubble is uniform. As seen from Fig. 1, regions 1 and 4 comprise much smaller part from the nebula than regions 2 and 3 do. Therefore, the plasma emissivity (or emission measure) of the X-ray emitting plasma is higher in regions 1 and 4, likely due to higher plasma density or higher concentration of clumps and filaments.

It is interesting to note that although we used simple plasma models to fit the observed X-ray spectra of NGC 6888, the derived abundances are fairly consistent between different models, and they are generally *inconsistent* with the typical abundances of a WN star (see below). In addition to the two basic models (2T *vaptec* and *vpshock*) used to fit the entire spectrum of NGC 6888, we ran some more complex ones: (i) a model with a distribution of thermal CIE plasma (we adopted our custom model which is similar to *cbpvmkl* in XSPEC but uses the *aptec* collisional plasma for the X-ray spectrum at a given temperature); (ii) a model with a distribution of adiabatic shocks with NIE effects taken into account (we made use of our custom model for XSPEC which was successfully used in the analysis of the X-ray spectra of SNR 1987A - e.g., Zhekov et al. 2009 and the references therein). We will discuss the result from these more complex models below (see § 4.2), and we only mention that the models with a distribution of CIE plasma or NIE shocks show two peaks in the distribution of their emission measure with temperature: one for a ‘cool’ plasma ($kT < 0.4$ keV) that dominates the X-ray emission from NGC 6888 and another for a ‘hot’ plasma ($kT \geq 2$ keV). The values for the plasma temperature of the 2T *vaptec* model are consistent with the values of the temperature peaks in the distribution of the CIE plasma.

For comparison, we also ran a *vpshock* model with a set of typical WN abundances (van der Hucht et al. 1986). We note that there was no good fit to the observed spectra unless we varied the abundances of N, O, Ne, Mg, and Fe. Figure 4 presents the derived abundances from various model fits to the entire X-ray spectrum of NGC 6888. All abundances are given with respect to the total number density of hydrogen and helium (H+He) which facilitates the comparison between cases with completely different basic set of abundances (e.g. solar vs. non-solar). On the one hand, this result illustrates the uncertainties of the derived abundances if using different plasma models and, on the other hand, it conclusively demonstrates that the chemical composition of the X-ray emitting plasma in NGC 6888 is quite different from that of the stellar wind of the central star in this object.

4.2. Very Hot Plasma in NGC 6888?

In order to search for indications of X-ray emission from hot plasma ($kT \geq 2$ keV), we expanded the photon range of interest and considered the X-ray spectra of NGC 6888 in the (0.3 - 4.0 keV) energy range. This increased the total number of source photons by $\sim 10\%$ compared to the (0.3 - 1.5 keV) spectra analyzed above. To improve the photon statistics, we re-binned the spectra to have a minimum of 200 counts per bin.

We used two models to fit the spectra: (i) one with a distribution of CIE plasma; (ii) and a model with a distribution of NEI shocks (as described in § 4.1). The quality of the fits was very good: $\chi^2/dof = 122/169$ (CIE plasma) and $\chi^2/dof = 120/168$ (NEI shocks). The derived values for the X-ray absorption and chemical abundances were entirely consistent with the values discussed in our analysis of the soft (0.3 - 1.5 keV) spectra. Figure 5 shows the NGC 6888 spectra overlaid with the best-fit model for a distribution of CIE plasma as well as the derived distribution of emission measure for the CIE plasma and NEI shocks.

We see that both models show a bi-modal distribution of the X-ray emitting plasma with peaks quite distinguished in the temperature space. The ‘cool’ plasma ($kT \leq 1$ keV) is the dominant source of X-ray emission in the (0.3 - 1.5 keV) energy range but provides only between (6 - 19)% of the flux at higher energies (1.5 - 4.0 keV), depending on the model used (e.g., CIE plasma or NIE shocks). It is thus quite likely that some hot plasma is present in the X-ray emitting region of NGC 6888. This plasma is needed to explain the weak but statistically significant emission (signal-to-noise $\sim 6 - 15$) in the (1.5 - 4.0 keV) energy range which may have been missed in the *ROSAT* and *ASCA* spectra of the entire WBB due to their considerably poorer photon statistics, and almost no sensitivity at energies ≥ 2 keV for *ROSAT*.

5. The Origin of the Hot Gas in NGC 6888

The two most important results from the model fits to the X-ray spectra of NGC 6888 that could be directly related to the origin of the hot gas in this object are: (i) the X-ray plasma in NGC 6888 has a relatively low temperature; (ii) the hot bubble abundances are not consistent with the ones of the stellar wind of the central star in NGC 6888 (see § 4).

The latter is justified in two ways as seen from Fig. 4. The X-ray abundances are smaller than the corresponding canonical WN values (typical for the central star) by (0.5 - 1.5) dex on the average. And, the N/O ratio derived from the analysis of the *Suzaku* data has a characteristic value of 2.0 - 3.0 which is much lower than the value of ~ 21.5 for the N/O ratio in the WN abundances set (e.g., van der Hucht et al. 1986). We note that low values

(~ 2) for the N/O ratio were derived from analysis of the optical emission of NGC 6888. Also, the N, O and Ne abundances derived from X-rays are very similar to those reported from the optical (Kwitter 1981; Moore et al. 2000; see also Fig. 4).

It is thus natural to conclude that the plasma which dominates the X-ray emission from NGC 6888 likely originates from the cold optical nebula. Subsequently, this cold plasma has been heated to high temperatures through a mechanism that is yet to be identified. This heating mechanism must be capable of explaining the relatively low plasma temperature in the hot bubble of NGC 6888 ($kT < 0.5$ keV; see § 4).

As proposed by the standard WBB model (Weaver et al. 1977; for numerical modeling see Zhekov & Myasnikov 1998), the electron thermal conduction is such a physical mechanism. Alternatively, the models of so called mass-loaded astronomical flows also suggest a relatively low temperature in the WBB objects (e.g., Hartquist et al. 1986; Arthur et al. 1993) but we note that it is not well established which is the actual physical mechanism that is responsible for the ‘instantaneous’ mixing of the hot bubble gas with the mass-loaded flow. In either case some important questions must find their answers in order to build a more complete global picture of NGC 6888.

Namely, what is the fate of the shocked stellar wind? Given the age of this WBB (§ 2), we note that the massive WN wind can supply up to one solar mass or so of hot gas with distinct non-solar abundances. How can we explain that we find no indications for such a plasma in the X-ray spectrum of NGC 6888? And, how can the presence of really high-temperature plasma ($kT \geq 2$ keV) fit into a general physical picture for WBB? Below, we will discuss these issues in some extent.

6. Discussion

6.1. Wind-Blown Bubble Hydrodynamics

In order to have a realistic view on the fate of the shocked WN stellar wind, we need to carry a direct comparison between the theoretical X-ray emission and the observed spectra of NGC 6888. For this goal, we adopted the following procedure. First, we used a 1D numerical hydrodynamic model to derive the distribution of plasma characteristics (temperature, density) in the hot bubble. In turn, we constructed the hot plasma distribution of emission measure with temperature. Second, we developed a custom model for XSPEC that uses thus derived distribution of emission measure to model the X-ray emission from NGC 6888. Finally, we used this model to fit the *Suzaku* spectra and check the consistency of the physical model with observations: e.g., whether the model provides correct observed

flux, abundances, X-ray absorption.

We briefly review some details about the WBB hydrodynamics (see Weaver et al. 1977 and numerical modeling in Zhekov & Myasnikov 1998). When a massive stellar wind interacts with the circumstellar matter, CSM, a two-slab structure will form, bounded by two shocks and a contact discontinuity separating the shocked CSM gas from the shocked stellar wind. During the evolution of this structure, its outer part will collapse due to the energy losses by emission and will appear as optical nebula. On the other hand, its inner part is not subject to significant energy losses due to its high temperature and low density but its structure will depend on the efficiency of the electron thermal conduction. In the case the thermal conduction is suppressed (e.g., due to presence of magnetic field), the hot bubble will remain adiabatic and it will contain only the very hot gas of the shocked stellar wind. Alternatively, the efficient thermal conduction will heat up part of the cold optical nebula which will expand inward (the contact discontinuity will move towards the inner shock). As a result, the plasma temperature in the hot bubble will decrease and its mass will increase. In this case the hot bubble will consist of two parts both filled with hot gas but with different chemical composition.

To derive the physical parameters of the hot bubble in NGC 6888, we used the 1D hydrodynamic code of A.V. Myasnikov that was developed for modeling the physics of a standard WBB (for details see Zhekov & Myasnikov 1998). This code allows modeling not only of adiabatic and radiative WBB but also of the case with efficient thermal conduction. It correctly handles interacting gas flows with different chemical compositions.

We adopted the following basic set of parameters that determine the physics of a WBB: (i) $\dot{M}_{WN} = 1.5 \times 10^{-5} M_{\odot} \text{ yr}^{-1}$ and $V_{WN} = 1600 \text{ km s}^{-1}$ for the stellar wind of the central star in NGC 6888 (see § 2); (ii) $\dot{M}_{sw} = 1.5 \times 10^{-4} M_{\odot} \text{ yr}^{-1}$ and $V_{sw} = 10 \text{ km s}^{-1}$ for the slow wind that has been emitted in the previous evolutionary stage of the central star. The interaction of such winds results in a WBB with a radius of $\sim 2.5 \text{ pc}$ at age of 30,000 years. We note that the size of the optical nebula NGC 6888 is $12' \times 18'$ (Chu et al. 1983; also see Fig. 1). Thus, a spherically-symmetric (1D) bubble with a radius of $\sim 2.5 \text{ pc}$ has the same volume as a prolate ellipsoid with major and minor axes equal to those of the optical nebula for the adopted distance to this object ($d = 1.26 \text{ kpc}$, § 2). With this approximation, we calculate the distribution of emission measure of the hot bubble and the corresponding normalization parameter for the model spectrum in XSPEC ($norm = 10^{-14} \int n_e n_H dV / 4\pi d^2$). Then, the actual spectral fit to the X-ray spectra can tell us if the theoretical emission measure gives the correct value for the observed flux from NGC 6888.

We fitted the total spectra of NGC 6888 with the theoretical X-ray emission for the case of conductive WBB having the basic set of physical parameters. In all model fits using

results from our hydrodynamic simulations, the abundances of the shocked stellar wind had values fixed to the typical WN abundances (van der Hucht et al. 1986) and only abundances of the ‘evaporated’ gas from the cold shell were allowed to vary. We note that using the basic set of parameters provided acceptable fit to the shape of the observed spectra but it grossly overestimated the observed flux (by a factor of ~ 50). To reconcile this flux discrepancy, it was necessary to reduce the amount of X-ray emitting plasma in the hot bubble. We ran a series of hydrodynamic simulations by simultaneously reducing the mass-loss rates of the central star in NGC 6888 and of the previously emitted slow wind which results in no change of the global geometry of the shock structure. In all these simulations, the wind velocities had their values as in the basic set of physical parameters (see above). The case with a reduction factor of ~ 4 for the mass-loss rates provided the correct observed flux and the derived abundances were a factor of (3 - 5) higher than the values in Fig. 4. The corresponding spectral fit ($\chi^2/dof = 266/238$) to the *Suzaku* spectra of NGC 6888 is shown in Fig. 6.

It is worth noting that although the required reduction for the mass-loss rates might seem considerable, we find additional evidence that this could well be the case. If we assume that the thermal conduction is not efficient and some other mechanism is responsible for the relatively low plasma temperature deduced from the analysis of the X-ray emission from NGC 6888 (§ 4), the hot bubble in this object will then be purely adiabatic. We ran a series of 1D hydrodynamic models for this case starting with the same set of basic physical parameters as described above. The result was that the shocked stellar WN wind plasma had too high a temperature and the models provided strong X-ray flux at energies > 1 keV considerably exceeding the one observed. For graphical clarity, we show in Fig. 6 the theoretical spectrum of purely adiabatic WBB with mass-loss rates reduced by a factor of 2. Note that the normalization (or the flux) of the theoretical spectrum scales with the mass-loss rate as $\propto \dot{M}^2$.

Therefore, it is conclusive that independently from which is the heating mechanism for the X-ray emitting plasma in NGC 6888, we find indications that the mass-loss rate of the central star should be smaller than the value of $\dot{M}_{WN} = 1.5 \times 10^{-5} M_{\odot} \text{ yr}^{-1}$ adopted here. Direct comparisons of the model predictions and the X-ray observations suggests a reduction factor of $\sim 3 - 4$.

6.2. General Physical Picture

A general physical picture of the X-ray emission from a WBB must provide a reasonable explanation about the origin of the X-ray emitting gas and the mechanism that heats it up

to the observed temperatures. Thus, we recall the basic properties of the X-rays from NGC 6888.

The previous observations of the entire WBB with *ROSAT* and *ASCA* found that the X-ray emission of NGC 6888 comes from clump-like structures (Wrigge et al. 1994; Wrigge et al. 2005). This is also the case as seen in the high signal-to-noise *Suzaku* data (Fig. 1). Our analysis of the *Suzaku* spectra of NGC 6888 showed that most of the X-rays come from relatively cool plasma ($kT \leq 0.5$ keV) but there is also some very hot plasma ($kT \geq 2$ keV; Fig. 5) that is responsible for the observed emission in the (1.5 - 4.0 keV) energy region.

The physical picture that emerges from the analysis of the X-ray data of NGC 6888 is then the following. Most of the soft X-rays come from clumps distributed in the hot bubble of this object. As indicated by the similar chemical composition of the X-ray emitting plasma and the optical shell (e.g., Fig. 4), these clumps likely originate from the cold but ionized optical nebula. Most probably they were formed through various dynamic instabilities the optical nebula was subject to during its evolution (e.g. see Garcia-Segura et al. 1996a; Garcia-Segura et al. 1996b; Stickland & Stevens 1998; and multiple shock waves may have contributed in the case of conductive WBB, Zhekov & Myasnikov 1998). In addition, there is some very hot plasma that can be associated with the shocked WN wind of the central star. The details of this general physical picture depend on the heating mechanism that operates in the hot bubble of NGC 6888.

Conductive WBB. If the electron thermal conduction is efficient, the energy of the shocked stellar wind will be dissipated, part of the outer shell will ‘evaporate’ and this will form a smooth component of relatively hot plasma filling in the inner part of the nebula. This case is well represented by the hydrodynamic model of WBB with thermal conduction and this model gave an acceptable fit ($\chi^2/dof = 266/238$) to the observed spectra (see § 6.1 and Fig. 6). In this picture, the dense ionized clumps that were formed via dynamic instabilities are engulfed by the hot bubble and heated up to X-ray temperatures thanks to the efficient thermal conduction. In fact, when we added an extra component (using model *vapex* in XSPEC) to the spectral fit based on the hydrodynamic simulations, the spectral model matched better the observed spectra ($\chi^2/dof = 232/238$) and the derived abundances had values consistent with those in Fig. 4. The derived plasma temperature for this additional component (the clumps) was $kT = 0.11 - 0.12$ keV. The main problem in the case of conductive WBB is that there cannot exist in the hot bubble plasma with temperatures as high as those derived from the fits to the *Suzaku* spectra in the (0.3 - 4.0 keV) energy range (§ 4.2 and Fig. 5). As a result, practically no photons are produced in the (1.5 - 4.0 keV) energy band contrary to what is observed (§ 4.2). We recall that *asymmetric*

thermal conduction (Zhekov & Myasnikov 2000) might be a remedy to this problem if a global ordered magnetic field is present in NGC 6888. Thus, there might be a small part in the hot bubble with a very hot plasma while the rest of it will be filled in with much cooler plasma. Unfortunately, the number of detected photons in the (1.5 - 4.0 keV) energy band did not allow us to study their spatial distribution and much deeper observations are needed for that purpose.

Adiabatic WBB. If the electron thermal conduction is suppressed due to the presence of magnetic field, the hot bubble will be adiabatic and the dense clumps that originate from the cold outer shell and penetrate the bubble interior are heated up to X-ray temperatures through some mechanism different from thermal conduction. We explored quantitatively this case by considering a spectral model consisting of two components: one representing the emission from the adiabatic hot bubble (from our hydrodynamic simulations) and another one (using model *vapex* in XSPEC) representing the X-ray emission of the dense clumps. We obtained a good fit ($\chi^2/dof = 183/237$) to the *Suzaku* spectra of NGC 6888 in the case of reduced by a factor of 3 mass-loss rates. The temperature of the dense clumps was $kT = 0.11 - 0.12$ keV and the derived abundances were consistent with those in Fig. 4. Then, what is the mechanism that heats up the dense clumps? Given the chemical composition of the clumps (or the cold nebula), shocks with velocity $\sim 300 - 350$ km s⁻¹ can provide the required temperature ($kT = 0.11 - 0.12$ keV). But, simple considerations show that the rarefied plasma in the hot bubble does not have the necessary power to run such shocks into a gas with much higher density than the hot plasma itself (e.g., given the stellar wind velocity of 1600 km s⁻¹, the expected relative velocity between the hot plasma and the clumps is maximum of the order of the velocity of the shock). Could it be that the dense clumps mix *locally* with the hot plasma and since the electron thermal conduction is inefficient, the energy exchange occurs directly between the heavy particles (ions) of the two components? Consequently, the electrons in the mixture are heated as well. Also, the relative velocity between the hot plasma and the clumps will favor such a diffusion of the heavy particles. We note that the adiabatic WBB does not have the high-temperature caveat of the conductive WBB mentioned above.

But, how can we distinguish between the two cases, conductive or adiabatic WBB? We think that there might be some observational differences resulting from these two heating mechanisms. The electron thermal conduction is a very efficient dissipative mechanism, thus the heating of the cold gas of the clumps will occur almost 'instantaneously'. On the other hand, the ion-ion energy exchange (thanks to diffusion of the hot ions into the cold gas) is much slower process. We recall that this different efficiency is due to the much faster energy exchange between the light particles (the characteristic time is proportional to the square root of the particle's mass; e.g., Spitzer 1962). Thus, we may expect that there will exist clumps

in the hot bubble that have temperature intermediate between that of the optical outer shell and the X-ray clumps. These clumps will be source of UV emission. Therefore, if spectral observations of NGC 6888 detect strong lines in the 1,000-2,000 Å spectral range (e.g., of ‘hot’ ions like NV, OVI), this will indicate that the thermal conduction is considerably suppressed in this object. Alternatively, if clumps with no strong UV emission are detected, this will favor the thermal conduction as the heating mechanism in NGC 6888. Another observational possibility also exists, although it is not quite feasible for the moment. Nordon et al. (2009) reported a narrow radiative recombination continuum (RRC) in the X-ray spectrum of the planetary nebula BD+60°3639. They interpret this RRC emission feature as result when bare C VII ions penetrating from the hot bubble into the cold optical nebula recombine with cool electrons. In general, the same can be expected when the hot ions diffuse into the cold clumps as proposed above and RRC of various ions can be expected. But, a crucial experiment for distinguishing between detection from non-detection of these RRC features must wait for future observations with the next generation of X-ray telescopes since such an experiment requires high spectral resolution X-ray observations which are not feasible for NGC 6888 at the moment.

All this, as well as the suggested reduction for the mass-loss rate of the central WN star, emphasizes the importance to carry out some global analysis of the entire system NGC 6888: central star, optical and X-ray nebula (hot bubble). Namely, a self-consistent modeling of the optical-UV emission of the central star (WR 136) and the optical nebula and confronting it with observations can provide us with a valuable piece of information about the wind velocity and mass loss, temperature distribution in the stellar wind, its abundances as well as the density and abundances of the optical nebula. This will put much tighter constraints on the physical parameters determining the physical conditions in the hot bubble (and its X-ray emission). In turn, it will result in a better constrained general physical picture of the whole system. A suitable example of adopting such a global approach in the analysis of the optical-UV emission of a complex system is given in Georgiev et al. (2008) for the case of the planetary nebula NGC 6543.

6.3. Ionization History of the Hot Plasma

The ionization history of the plasma in the hot bubble of a WBB is quite complex. Consider the standard WBB model. In this case, the thermal conduction is efficient and we have two parts in the hot bubble filled correspondingly with the shocked stellar wind and the evaporated gas from the cold optical nebula. During the evolution of the WBB, the temperature in the hot bubble decreases with time as well as does its density. Thus, each

new parcel of gas, crossing the inner shock or evaporating from the cold nebula, will have its own ionization history. This will depend on the time that parcel of gas entered the hot bubble, that is on the physical parameters of the hot plasma and their subsequent evolution until the moment of observations. We note that it is likely (although it depends on the physical parameters for each studied object) that the plasma on both sides in vicinity of the contact discontinuity will be almost in CIE while that close to the inner shock or to the outer boundary in cold nebula will be in state of NEI. In purely adiabatic WBB, the ionization history of the plasma is similar but then the hot bubble contains only the shocked stellar wind. This picture becomes even more complicated in objects like NGC 6888 where the X-ray emission is not spatially uniform which indicates a presence of clump like structures.

Unfortunately, it is not feasible to follow the ionization history of the plasma in the hot bubble in the theoretical models or to deduce valuable information about it from the X-ray observations. The latter is particularly valid for the case of CCD X-ray spectra. For that reason, our approach in this study was to consider two limiting cases: plasma models with CIE and models that, although in a simplified but well defined manner, take into account the NEI effects. Such an approach illustrates better the uncertainties in the derived properties (e.g., temperature, abundances, emission measure) of the X-ray emitting plasma.

7. Conclusions

In this work, we presented an analysis of the *Suzaku* data on NGC 6888: the wind-blown bubble around the Wolf-Rayet star WR 136. For the first time, X-ray spectra of the entire nebula are obtained that have a very good quality allowing a detailed comparison between theory and observations. The basic results and conclusions are as follows.

1. The X-ray spectra of the WBB NGC 6888 are soft and most of the emission is in the (0.3 - 1.5 keV) energy range although some emission ($\sim 10\%$ of the observed flux) is found at higher energies (1.5 - 4.0 keV). The spectral fits require a relatively cool plasma with $kT \leq 0.5$ keV but much hotter plasma with temperature $kT \geq 2.0$ keV is needed to match the observed hard X-ray emission. We find no appreciable temperature variations within the hot bubble of NGC 6888.
2. One of the important results from the spectral fits is that the derived abundances (N, O, Ne) are very much the same as those of the optical nebula. Also, they are considerably different from the WN abundances (van der Hucht et al. 1986) assumed ‘typical’ for the wind of the central star in the nebula. This indicates a common origin of the X-ray emitting gas and the outer cold shell, that is most of the X-ray plasma

(likely concentrated in clumps as the X-ray images indicate) has flown into the hot bubble from the optical nebula.

3. A direct comparison (in XSPEC) between 1D hydrodynamic models and the X-ray spectra of NGC 6888 suggests a reduced mass-loss rate ($\sim 4 - 5 \times 10^{-6} M_{\odot} \text{ yr}^{-1}$) of the central star in order to provide the correct value of the observed flux. We note that this figure is appreciably low for Wolf-Rayet stars and thus emphasizes the need of a global modeling of the entire system: central star, optical nebula and the hot bubble.
4. The general physical picture that emerges from the current analysis is the following. Most of the X-rays come from clumps distributed in the hot bubble of NGC 6888. These clumps originate from the cold optical nebula and they formed through various dynamic instabilities during the evolution of the wind-blown bubble. The shocked WN wind of the central star is likely the source of the very hot plasma ($kT \geq 2 \text{ keV}$) in this wind-blown bubble. If the electron thermal conduction is efficient, this can naturally explain the relatively low plasma temperature of most of the X-ray emitting plasma. Alternatively, the hot bubble in NGC 6888 will be adiabatic and the cold clumps are heated up to X-ray temperatures likely by energy exchange between the heavy particles (e.g., a local diffusion of the rarefied hot plasma into the dense clumps).

This work was supported by NASA through the NASA Goddard award NNX09AW39G to the University of Colorado at Boulder. The optical image in Fig. 1 is based on photographic data of the National Geographic Society – Palomar Observatory Sky Survey (NGS-POSS) obtained using the Oschin Telescope on Palomar Mountain. The NGS-POSS was funded by a grant from the National Geographic Society to the California Institute of Technology. The Digitized Sky Survey was produced at the Space Telescope Science Institute under US Government grant NAGW-2166. The authors thank an anonymous referee for his/her comments and suggestions.

Facilities: *Suzaku* (XIS).

REFERENCES

- Abbott D.C., Biegging J.H., Churchwell E., Torres A.V. 1986, ApJ, 303, 239
- Allen, C.W. 1973, Astrophysical Quantities, University of London, The Athlone Press
- Anders E., Grevesse N., 1989, Geochimica et Cosmochimica Acta, 53, 197

- Arnaud, K.A. 1996, in Jacoby G., Barnes, J. eds., ASP Conf. Ser. Vol. 101, Astronomical Data Analysis Software and Systems, Astron. Soc. Pac., San Francisco, 17
- Arthur, S.J., Dyson, J.E. & Hartquist, T.W. 1993, MNRAS, 261, 425
- Bochkarev, N.G. 1988, Nature, 332, 518
- Brighenti, F., & D’Ercole, A.D. 1995a, MNRAS, 273, 443
- Brighenti, F., & D’Ercole, A.D. 1995b, MNRAS, 277, 53
- Brighenti, F., & D’Ercole, A.D. 1997, MNRAS, 285, 387
- Chu, Y.H., Treffers, R.R., & Kwitter, K.B. 1983, ApJS, 53, 937
- Chu, Y.H., Guerrero, M.A., Gruendl, R.A., Garcia-Segura, G., & Wendker, H.J. 2003, ApJ, 599, 1189
- Chu, Y.H., Gruendl, R.A., & Guerrero, M.A. 2006, Proceedings of the X-ray Universe 2005 (ESA SP-604), editor A.Wilson, 363
- D’Ercole, A.D. 1992, MNRAS, 255, 572
- Dyson, J.E. 1982, in Investigating the Universe, ed. Kahn F.D., Riedel Publishing Co., Dordrecht, Holland, 125
- Falle, S.A.E.G. 1975, A&A, 43, 323
- Garcia-Segura, G., & Mac Low, M.-M. 1995b, ApJ, 455, 160
- Garcia-Segura, G., Langer, N., & Mac Low, M.-M. 1996, A&A, 316, 133
- Garcia-Segura, G., Mac Low, M.-M., & Langer, N. 1996, A&A, 305, 229
- Georgiev, L.N., Peimbert, M., Hillier, D.J., Richer, M.G., Arieta, A., & Peimbert, A. 2008, ApJ, 681, 333
- Hartquist, T.W., Dyson, J.E., Pettini, M., & Smith, L.J. 1986, MNRAS, 221, 715
- Kwitter, K.B. 1981, ApJ, 245, 154
- Lozinskaya, T.A. 1982, Ap&SS, 87, 313
- Lozinskaya, T.A. 1992, Supernovae and Stellar Wind in the Interstellar Medium, New York, American Institute of Physics

- McCray, R. 1983, in *Highlights of astronomy*, 6, 565
- Moore, B.D., Hester, J.J., & Scowen, P.A. 2000, *AJ*, 119, 2991
- Nordon, E., Behar, E., Soker, N., Kastner, J.H., & Yu, Y.S. 2009, *ApJ*, 695, 834
- Panagia, N. & Felli, M. 1975, *A&A*, 39, 1.
- Pikelner, S.B. 1968, *Astrophysical Letters*, 2, 97
- Prinja, R.K., Barlow, M.J., & Howarth, I.D. 1990, *ApJ*, 361, 607
- Rozyczka, M. 1985, *A&A*, 143, 59
- Rozyczka, M., & Tenorio-Tagle, G. 1985a, *A&A*, 147, 202
- Rozyczka, M., & Tenorio-Tagle, G. 1985b, *A&A*, 147, 209
- Rozyczka, M., & Tenorio-Tagle, G. 1985c, *A&A*, 147, 220
- Skinner S.L., Zhekov S.A., Güdel M., Schmutz W. & Sokal, K.R. 2010, *AJ*, 139, 825
- Spitzer, L. 1962, *Physics of Fully Ionized Gases* (New York: Interscience)
- Stickland, D.K., & Stevens, I. 1998, *MNRAS*, 297, 747
- van der Hucht, K.A. 2001, *New Astronomy Rev.*, 45, 135
- van der Hucht, K.A., Cassinelli, J.P., & Williams P.M. 1986, *A&A*, 168, 111
- Weaver, R., McCray, R., Castor, J., Shapiro, P., & Moore, R. 1977, *ApJ*, 218, 377
- Wrigge, M. 1999, *A&A*, 343, 599
- Wrigge, M., Wendker, H.J., & Wisotzki, L. 1994, *A&A*, 286, 219
- Wrigge, M., Vhu, Y.-H., Magnier, E.A., & Wendker, H.J. 2005, *ApJ*, 633, 248
- Wright, A.E. & Barlow, M.J. 1975, *MNRAS*, 170, 41
- Zhekov S.A., McCray, R., Dewey, D., Canizares, C.R., Borkowski, K.J., Burrows, D.N. & Park, S. 2009, *ApJ*, 692, 1190
- Zhekov S.A., & Myasnikov, A.V. 1998, *New Astronomy*, 3, 57
- Zhekov S.A., & Myasnikov, A.V. 1998, *ApJ*, 543, L53

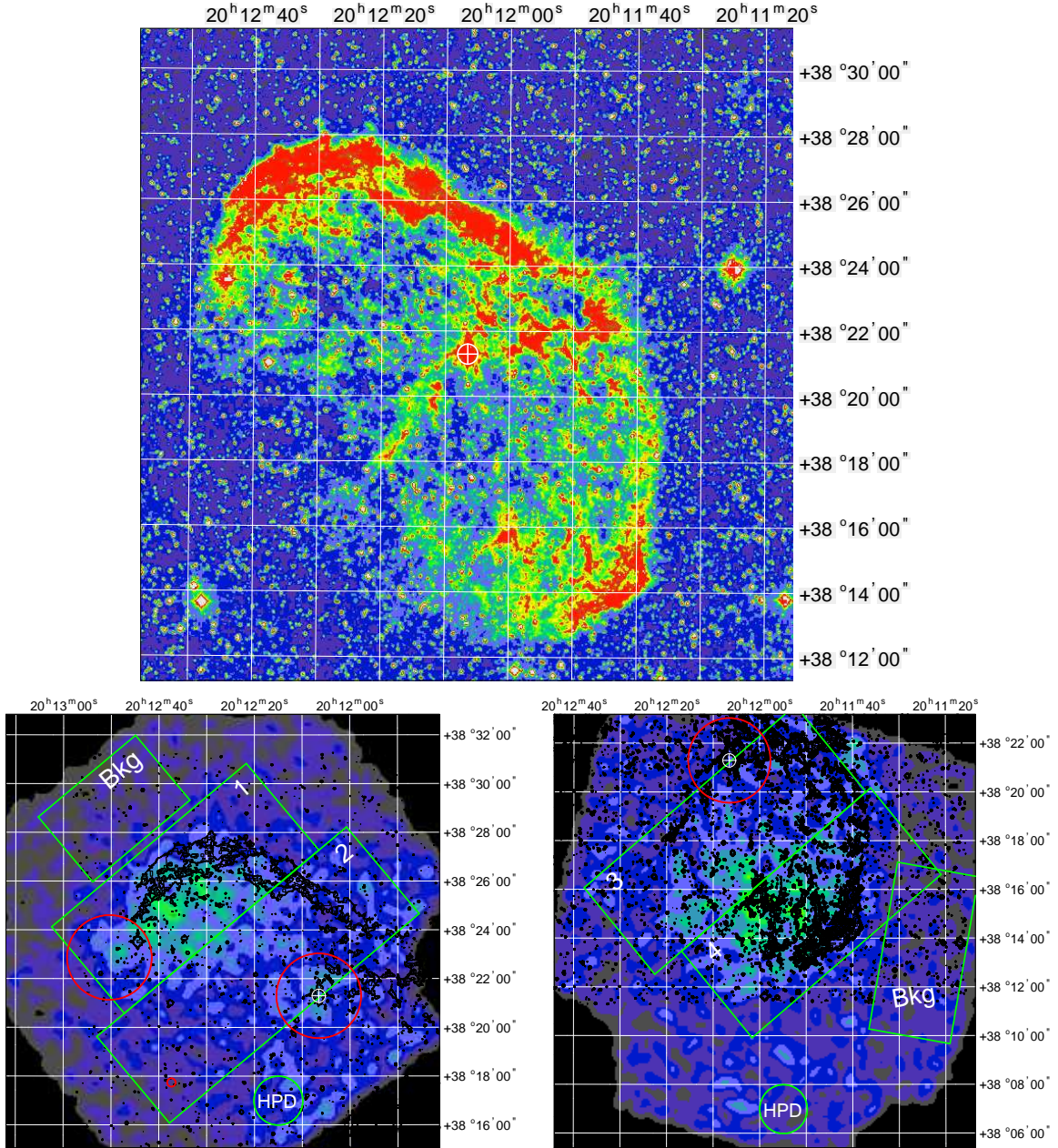


Fig. 1.— NGC 6888 images: optical (Palomar Observatory Sky Survey; upper panel); *Suzaku* XIS1 (0.3 – 4.0 keV) for the June 2009 (lower left panel) and November 2009 (lower right panel) observations. R.A. (J2000) and decl. (J2000) are on the horizontal and vertical axes, respectively. The boxes in green denote the extraction regions for the source (numbered from 1 through 4) and background spectra (labeled ‘Bkg’). The circles in red mark the regions around point sources that were excluded from the spectral extraction. The circled plus sign gives the position of the central star WR 136 in NGC 6888. In lower panels, the circle in green (labeled ‘HPD’) illustrates the half-power diameter (~ 2 arcmin) of the *Suzaku* telescopes. The X-ray images are re-binned (4×4 original pixels) and wavelet smoothed for presentation. For clarity, overlaid are some contours (in black) of the optical image. Note that the lower panels show the *raw* X-ray images, thus, their brightness scale is different due to the different non X-ray background.

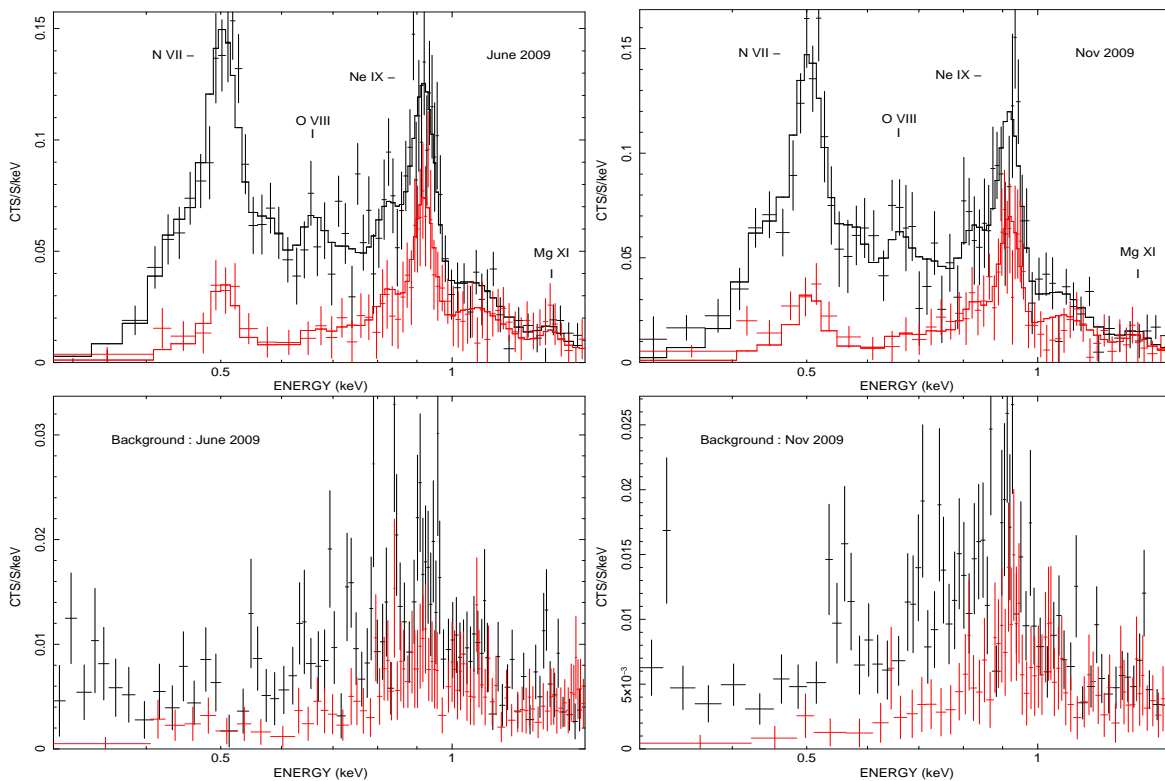


Fig. 2.— NGC 6888 background-subtracted spectra overlaid with the best-fit 1T shock model (Table 1). In each upper panel, the XIS1 spectrum is in black and the XIS0+3 spectrum is in red (lower curve). The North-East and South-West halves of the bubble were observed correspondingly in June and November 2009. For comparison, the lower panels show the corresponding background spectra after subtracting the non X-ray background.

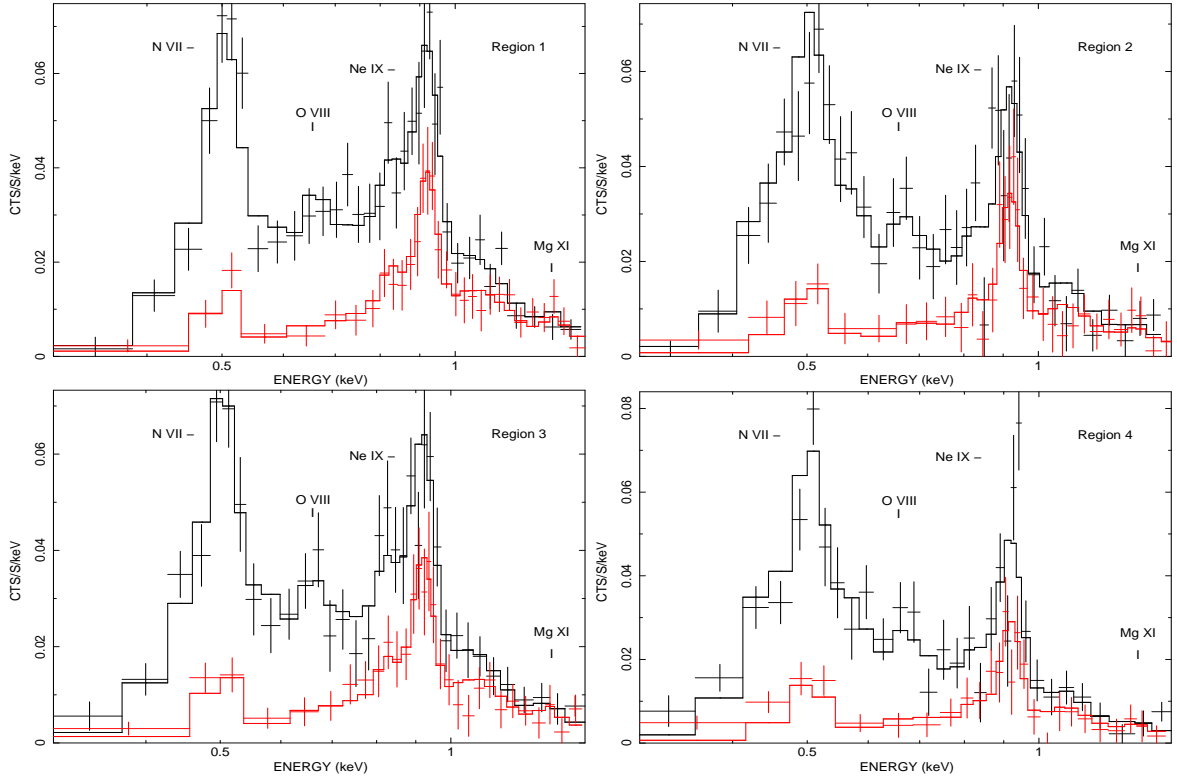


Fig. 3.— NGC 6888 background-subtracted spectra from the four extraction regions in Fig. 1 overlaid with the best-fit 1T shock model. In each panel, the XIS1 spectrum is in black and the XIS0+3 spectrum is in red (lower curve).

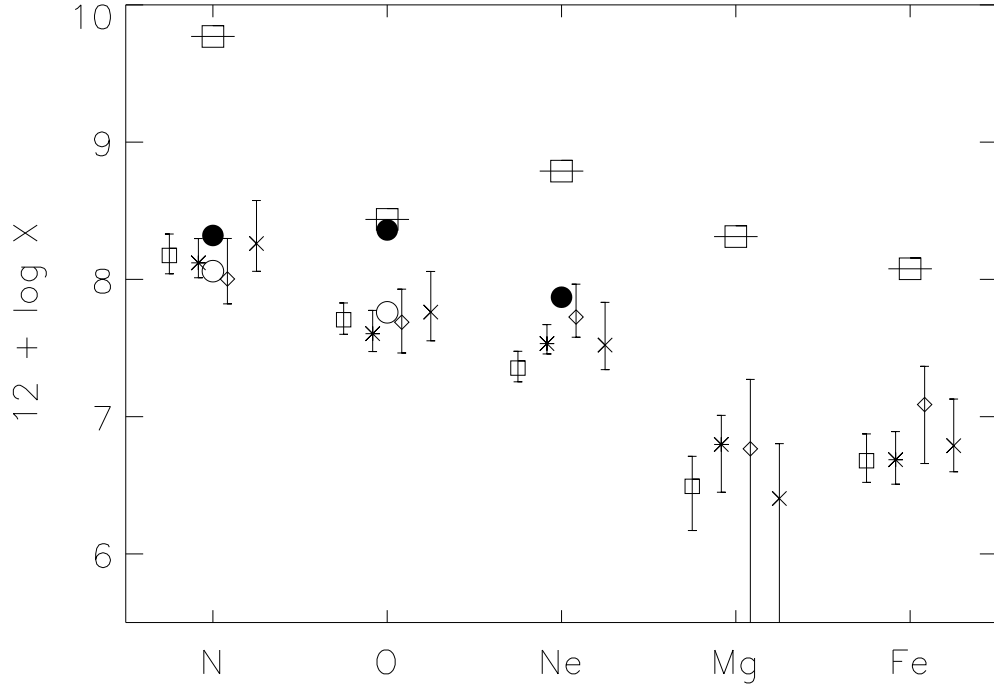


Fig. 4.— The abundance values of N, O, Ne, Mg and Fe derived from the global model fits to the entire X-ray spectrum of NGC 6888 . The abundance values are with respect to the total number density of H+He and in units of $12 + \log X$ (X is any of N, O, Ne, Mg and Fe). The symbols with error bars denote results from the fits with *vpshock* and solar abundances - squares; *vpshock* and WN abundances - asterisks; distribution of CIE plasma - diamonds (the values from the 2T *vapec* model fits are not given since they are within the plotted error bars); distribution of NEI shocks - crosses. Errors are 1σ values from the fits. The abundances values derived from analysis of the optical data by Kwitter (1981) and Moore et al. (2000) are shown with filled and empty circles, respectively. For reference, the *typical* abundances of WN stars (van der Hucht et al. 1986) are given by empty squares with horizontal bars (these bars have no meaning and are used only for graphical clarity).

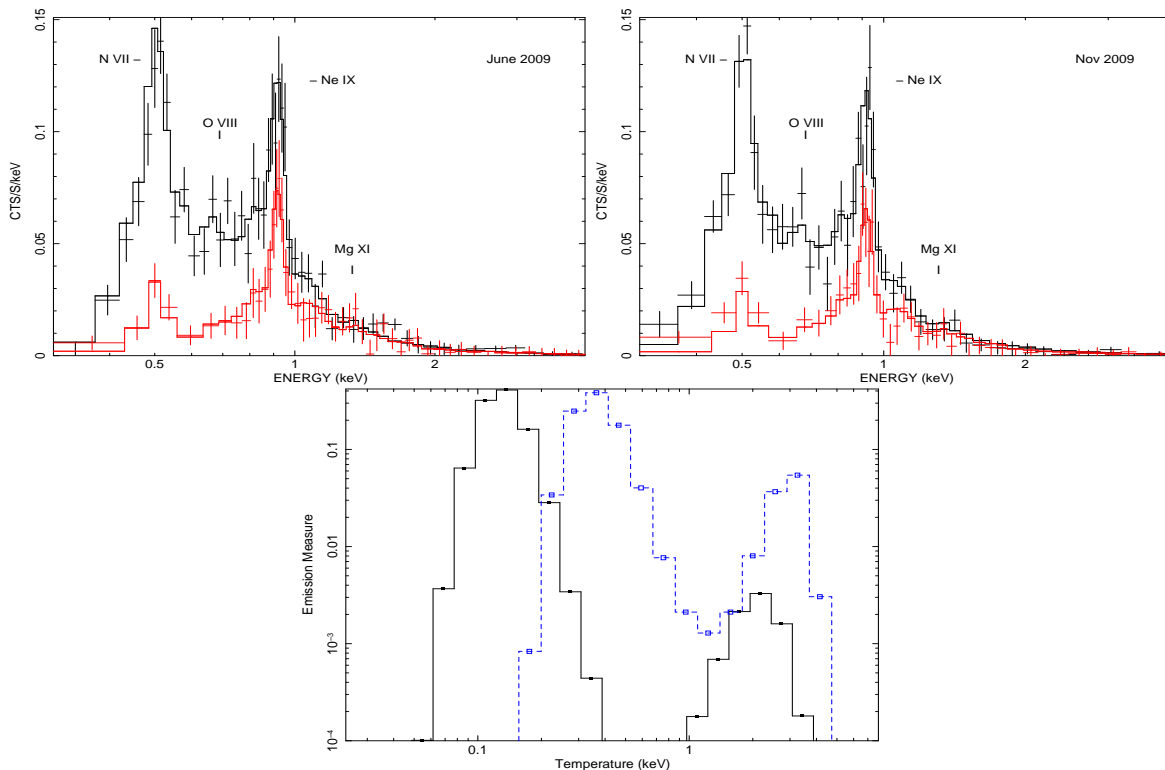


Fig. 5.— The (0.3 - 4.0 keV) background-subtracted spectra of NGC 6888 (re-binned to have a minimum of 200 counts per bin) overlaid with the best-fit model with a distribution of CIE plasma. In each panel, the XIS1 spectrum is in black and the XIS0+3 spectrum is in red (lower curve). The derived distribution of emission measure (normalized to have a total sum of unity) is shown in the third panel: that of the CIE plasma in black (solid line) and the one of the NEI shocks in blue (dashed line).

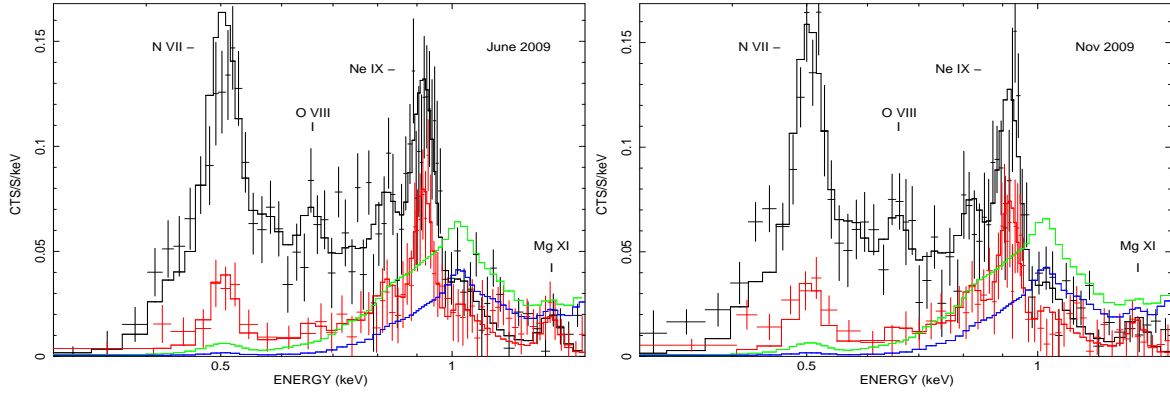


Fig. 6.— NGC 6888 background-subtracted spectra as in Fig. 2 overlaid with the best-fit model from the 1D hydrodynamic simulations for conductive WBB with mass losses reduced by a factor of ~ 4 . In each panel, the XIS1 spectrum is in black and the XIS0+3 spectrum is in red (lower curve). For comparison, the model spectra from a purely adiabatic WBB are shown in green (XIS1 spectrum) and blue (XIS0+3 spectrum). See text for details.

Table 1. Global Spectral Model Results

Parameter	2T vapec	vpshock
χ^2/dof	172/232	177/235
N_H (10^{21} cm $^{-2}$)	$1.92^{+0.42}_{-0.44}$	$2.07^{+0.47}_{-0.46}$
kT $_1$ (keV)	$0.15^{+0.01}_{-0.01}$	$0.48^{+0.22}_{-0.11}$
kT $_2$ (keV)	$2.03^{+1.31}_{-0.52}$
EM $_1$ (10^{55} cm $^{-3}$)	$80.8^{+25.6}_{-16.6}$	$6.3^{+3.3}_{-1.8}$
EM $_2$ (10^{55} cm $^{-3}$)	$1.0^{+0.17}_{-0.14}$
Abundances	Varied	Varied
τ (10^{10} cm $^{-3}$ s)		$3.98^{+2.85}_{-1.52}$
F_X (10^{-12} ergs cm $^{-2}$ s $^{-1}$)	2.05 (18.4)	1.92 (17.4)

Note. — Results from simultaneous fits to the XIS1 and XIS0+3 spectra of NGC 6888 from the *Suzaku* observations in June and Nov 2009. Tabulated quantities are the neutral hydrogen absorption column density (N_H), plasma temperature (kT), emission measure ($\text{EM} = \int n_e n_H dV$), shock ionization time-scale ($\tau = n_e t$), the X-ray flux (F_X) in the 0.3 - 1.5 keV range followed in parentheses by the unabsorbed value. Only abundances of N, O, Ne, Mg and Fe were varied in the fits (see Fig. 4). Errors are the 1σ values from the fits.